Synthesis of Energy Producing Material by Liquid Phase Epitaxy

Pankaj Kumar[*1], Ayush Kumar[*2]

[#]*Research Scholar, Department of Energy Science and Engineering, Indian Institute of Technology Bombay Mumbai-400076, India*
[*]*Scientist, Indian Space Research Organization, Ahmedabad-380058, India*

Abstract—*Hybrid Halide Perovskite materials are most promising solution for optoelectronic devices due to several inherent properties such as long range crystallinity, high carrier mobility, large diffusion length of charge carrier, ease solution processability, low cost, high absorption coefficient and so on. The liquid phase epitaxy growth of these materials and their different optical and structural characterization is presented in the present work. LPE is the growth of thin film from supersaturated solution of material. We use different substrate for LPE deposition to get long order crystallinity in film along with good coverage and uniformness of surface. Literature review on electronic, structural and optical properties of hybrid perovskite materials is also presented.an overviewof various growth techniques for liquid phase epitaxy is also presented.*

Keywords —*Perovskite solar cell, Liquid phase epitaxy (LPE)*

I. INTRODUCTION

Perovskite solar cells are recent breakthrough in solution based, low cost photovoltaics. It can be also flexible and colourful. Its power conversion efficiency is fastest grown in the history of any solar cell technology. The PCE of perovskite solar cells approached more than 23 % only in seven years from 3.8 % in 2009.In 2006 Miyasaka *et.al* used $CH_3NH_3PbBr_3$(Akihiro Kojima, 2009) as a sensitizer in dye sensitized solar cell, PCE was found 2.6% and in 2009 with replacing $CH_3NH_3PbBr_3$ with $CH_3NH_3PbI_3$, the PCE was found 3.8 %. First stable solid state solar cell was introduced in mid-2012 when liquid junction is replaced by solid spiro-MeOTAD as a hole-transporting layer (Kim et al. 2012). Using similar mesoscopic-structure architecture, Lee and Snaith et al. achieved an efficiency of 7.6 %(Liu et al. 2013). Replacing electrically conducting TiO_2 with electrically inert Al_2O_3, they found that efficiency increased to 10.9%. Though they were uncertain that whether Al_2O_3 performs better than TiO_2, but result concludes to that perovskite is itself a good charge transporter.

II. PROPERTIES OF HYBRID HALIDE PEROVSKITES

In this section, we report different properties of Hybrid Halide Perovskite materials. This section also consists of literature review of previous works. These materials are benefited from excellent optoelectronic properties such as a high and balanced carrier mobility, long carrier diffusion length, large light absorption coefficient in the UV–vis range tunable optical properties and low excitonic binding energy.

A. Structural properties of hybrid halide perovskite

Halide Perovskite is the general name of materials with chemical formula ABX_3, where A^+, B^{++} are cations and X^- is anion.
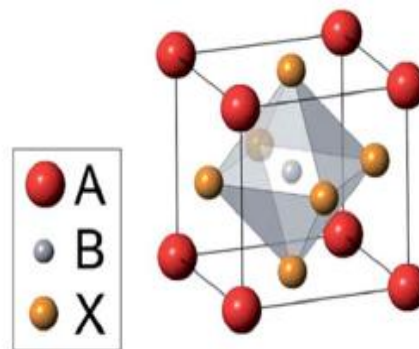
Fig. 1structure of perovskitematerial(Luo & Daoud 2015)

In case of organic-inorganic halide perovskite A^+ is organic cation, B^{++} is inorganic cation and X^- is halide anion. There are pure $CH_3NH_3PbX_3$ and mixed perovskite $CH_3NH_3PbX_{3-z}Y_z$, where X and Y= I, Br, Cl and z is the composition Y in mixed perovskite. Mixing different composition of Y, we can tune the bandgap material.Perovskite exists in three phases, namely cubic phase (α phase), tetragonal phase (β phase) and orthorhombic (γ phase). In cubic phase organic cation (A^+) occupy the eight corner of the cube and each cation have 12 nearest neighbour halide anion, whereas inorganic cation (B^{++}) occupy body centre and have 6 nearest neighbour halide anion.

$CH_3NH_3PbX_3$	lattice parameters (Å)	Calculated band gap	Room temperature structure
X=I	a = 6.33	1.57	Tetragonal
X=Br	a = 5.90	1.80	Cubic

X=Cl	a = 5.68	2.34	Cubic

B^{++} and six halide anion form octahedral void. Their crystallographic stability and probable structure can be deduced by considering a tolerance factor (t) and an octahedral factor (μ) (Chonghea Li, 2008). Tolerance factor (t) is defined as $\frac{R_A + R_X}{\sqrt{2}*(R_B + R_X)}$ and octahedral factor (μ) as $\frac{R_B}{R_X}$, where R_A, R_B and R_X are radius of A, B and X ions respectively. In general range of these are 0.81< t<1.11 and 0.44<μ< 0.90. If t lies between 0.89 and 1.0 then perovskite obtain the cubic structure. Smaller t (<0.81) leads to lower symmetry tetragonal (β phase) or orthorhombic (γ phase) structures, whereas larger t (t > 1) could destabilize the three dimensional (3D) B–X network, leading to a two-dimensional (2D) layer structure.

B. Electronic Structure

T. Umebayashi *et. al.*(E. Mosconi, 2013)using ultraviolet photoelectron spectroscopy and first principles density functional theory (DFT) band calculations for the room temperature cubic phase 3D $CH_3NH_3PbI_3$found that valence band is maxima comprises the Pb 6s – I 5p σ-antibonding orbital, while the conduction band minima consists of Pb 6p – I 5s σ anti-bonding and Pb 6p – I 5p π anti-bonding orbitals.
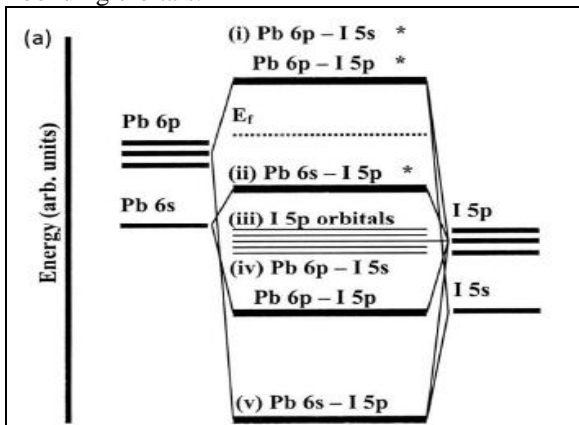
Fig. 2 Bonding diagram of [PbI6]4- cluster showing valence band (Pb 6p – I 5p σ*), conduction band (Pb 6p – I 5s σ*and Pb 6p – I 5p π*) and Fermi level (Mathews, 2014).

$CH_3NH_3PbX_3$ perovskites exhibited the expected absorption blue shift (increase in band gap) along I → Br → Cl series (Edoardo Mosconi, 2013). It was observed that bandgap energy of perovskite is mainly determined by $[PbI_6]^{4-}$ network, organic $CH_3NH_3^+$ ion have very little influence on bandgap energy.

C. Exitonic and free charge carrier properties

Temperature dependence of optical absorption of $CH_3NH_3PbI_3$ and $CH_3NH_3PbI_{3-x}Cl_x$ thin film for temperature range 4.2 K to 290 K are shown figure below.
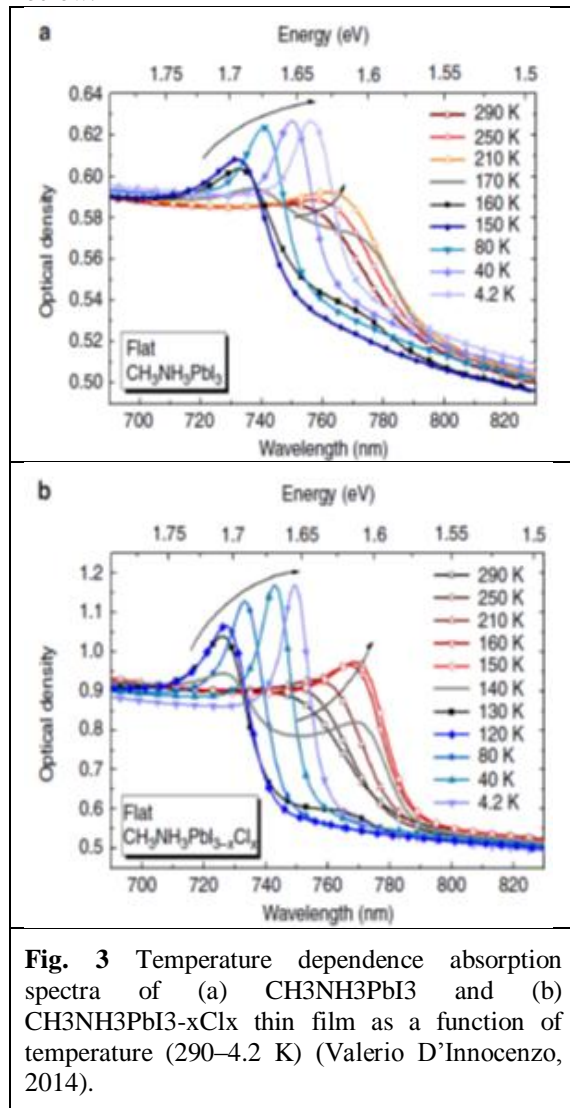
Fig. 3 Temperature dependence absorption spectra of (a) CH3NH3PbI3 and (b) CH3NH3PbI3-xClx thin film as a function of temperature (290–4.2 K) (Valerio D'Innocenzo, 2014).

A sharp peak at ~765nm emerges at lower temperatures was observed, which was attributed to an excitonic transition (Valerio D'Innocenzo, 2014).At 170K, a second excitonic peak emerges at 740 nm. Continuous temperature reduction result in shift of latter peak to longer wavelength side and increase in intensity while former peak disappears. This behaviour is attributed to a phase transition of the perovskite crystal, from a tetragonal to an orthorhombic structure, which begins at 170 K, inducing a blue shift in the absorption edge of about 60 meV, and completes at 150 K.At room temperature, excitonic peak and conduction band continuum are become indistinguishable.Exciton binding energy in the organo-lead mix-halide perovskite is 55±20 meV. This energy is comparable to solar cell operation thermal energy. This indicates that free charges are predominantly

generated and are responsible for PV operation following light absorption (Valerio D'Innocenzo, 2014).

III. LIQUID PHASE EPITAXY (LPE) GROWTH

Epitaxy is word originated from Greek word 'epi' and 'taxis'refers to the deposition of a crystalline overlayer on a crystalline substrate. The deposited layer is called an epitaxial film or epitaxial layer.Epitaxial films may be grown from gaseous or liquid precursors. Depending on precursor's different type of epitaxial growth are Liquid Phase Epitaxy (LPE), Vapour Phase Epitaxy (VPE), Molecular Beam Epitaxy (MBE), and Metal Organic Chemical Vapour Decomposition (MOCVD).

LPE is growth of material from supersaturated solution at high temperature or diluted solutions at low temperature (peter & Michael, 2007).LPE applied to many compounds but main applications are compound semiconductor such as GaAs, AlAs and YBCO for their application in laser, LED and other optoelectronic devices.

A. Epitaxial growth modes

There are eight modes of epitaxy growth including three well known modes Volmer-Weber, Stranski-Krastanov, Frank-Van der Merwe, columnar growth, step flow mode, step bunching, and screw-island or spiral island growth, and the growth on kinked (rough) surfaces. The surface coverage and uniformity is strongly dependent on growth mode. The growth mode is determined by relative magnitude of surface free energy of epilayer and interfacial energy between epilayer and substrate. For dominating interfacial energy between substrate and epilayer, Frank – Van der Merwe mode adopted. While Volmer-Weber mode (Volme-Weber, 1926) for the weakest interfacial energy, and Stransk-Krastanov (Stranski – Krastanov, 1938) as the intermediate case.

In the *layer-by-layer* or *Frank–Van der Merwe* growth mode first few steps are nucleated at different site of surface then these step grow laterally until they coalescence with other nuclei and form a monolayer of desired material then formation of next layer takes place continues. Nucleation for next layer happens only when previous monolayer completes.

In Volmer–*Weber* growth mode Process starts with nucleation then formation islands and growth of islands and finally islands coalescence with each other. In contrast with F-VM mode, it is columnar growth and always leaves the surface non-uniformity. The *Stranski–Krastanov* mode is the intermediate between the F-VM and V-W modes. Generally, found on substrate with small lattice constant difference from growing film. At initial stage, due to relatively large substrate-epilayer interface energy, first one or two compact monolayers are formed onto which by surface nucleation, but after that due to increasing misfit with substrate surface island formation starts and follows the V-W growth mechanism.

In LPE, *step bunching* is observed at high supersaturation solution. In this case high density of steps grows with large step velocities over the surface see figure 4.

B. Thin film growth rate

When supersaturated solution is moved onto substrate and then reducing the temperature, solute in vicinity of substrate get deposited on substrate and a solute depleted layer of is formed above the substrate. Due to concentration difference between bulk solution and

solution in vicinity of substrate solute atoms diffuses through the depleted layer (δ). Diffusion through this solute depleted layer define the film growth rate and given by (peter & Michael, 2007).

$$v = (n\text{-}n_e)\ D/\rho\delta$$

Where n is effective concentration of solute, n_e the equilibrium conc. of solute, D is the diffusion coefficient and ρ the density of deposited film.
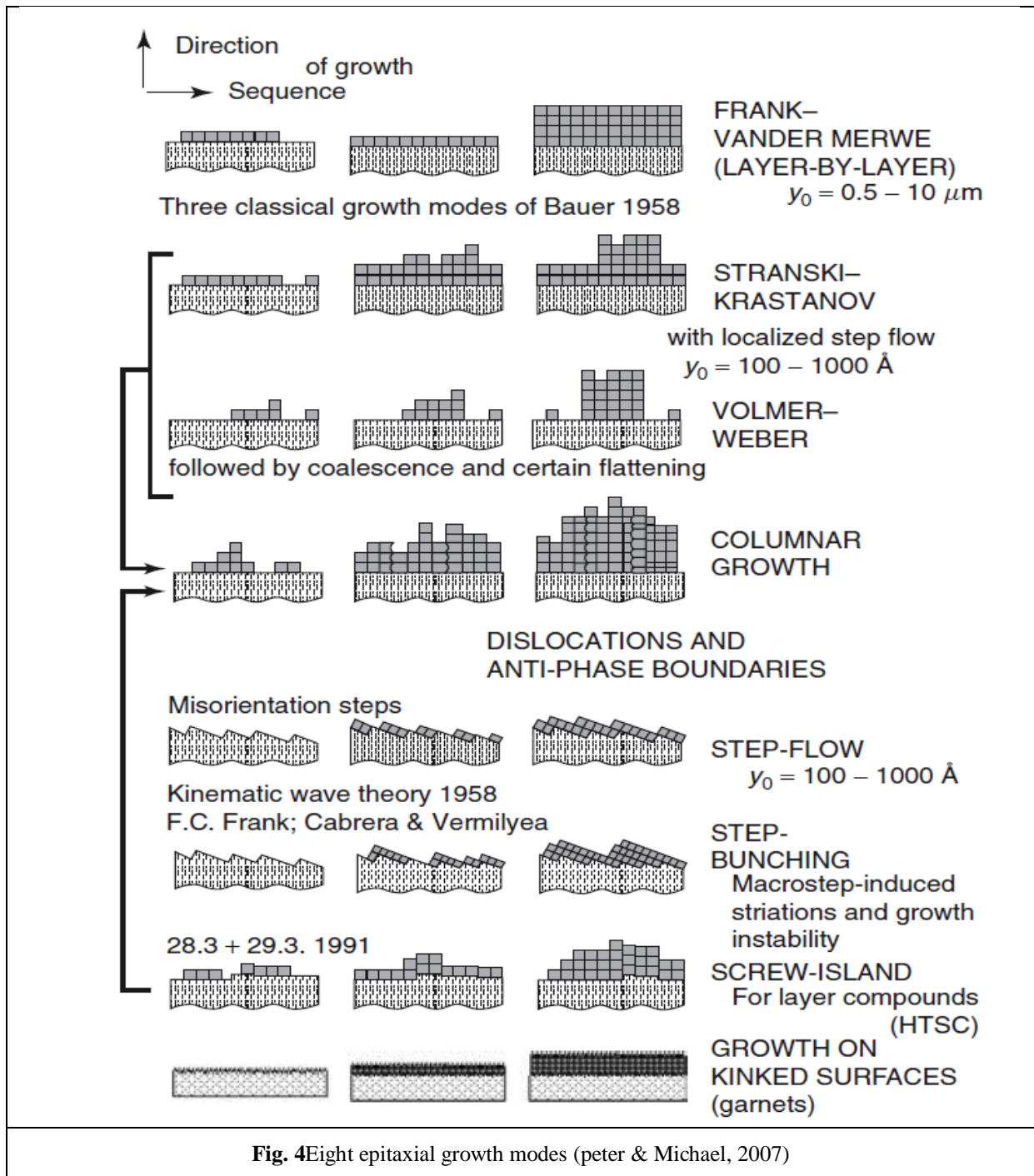
Fig. 4 Eight epitaxial growth modes (peter & Michael, 2007)

Increasing supersaturation increases the film growth rate, but high supersaturation also increases the instability, good quality film growth and step bunching, wavy macro steps, formation of inclusions, edge nucleation and surface dendrites, hopper growth and bulk dendrites are observed. Hence there is a maximum stable growth rate given by (peter & Michael, 2007)

$$v= \{0.214\ D\ u\sigma^2 n^2_e/Sc^{1/3}\rho^2 L\}^{1/2}$$

Where　u= solution flow rate
$\sigma=(n-ne)/ne$ =relative supersaturation.

L = crystal size or substrate diameter
$Sc = h/\rho_1 D$, h=dynamic viscosity and

ρ_1= density of the liquid

High density of screw islands (or spiral islands) is formed in screw island mode. The density of these islands corresponds are typically 10^8 -10^9 cm^{-2} and is dependent on initial nucleating sites. It is suggested that this growth mode originates due to coalescence of slightly misoriented islands.

IV. LIQUID PHASE EPITAXY GROWTH TECHNIQUES

Supersaturation obtained by cooling the growth solution from saturate solution at higher temperature provides the driving force of LPE growth. Supersaturation can be stablished in three ways.

(a)Ramp (or equilibrium) cooling,
(b) step-cooling &
(c) super-cooling technique.

In ramp-cooling, temperature is decreased at a constant rate. While in step-cooling technique, the temperature is reduced rapidly to obtain a large supersaturation.
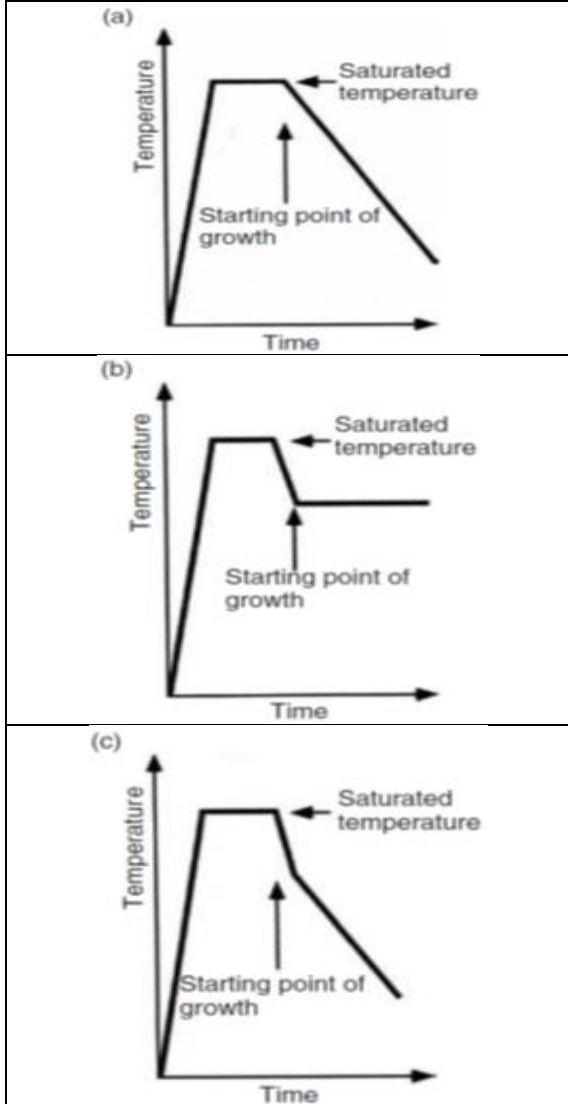
Fig.5 Cooling processes of LPE: (a) ramp-cooling; (b) step-cooling; (c) super-cooling (peter & Michael, 2007)

Rapid cooling also reduces the chance of substrate dissolution in solution, while super-cooling technique has advantage of both the ramp- and step cooling techniques. At first, rapid cooling attained for large supersaturation, and then film is grown at a constant cooling rate.

There are namely four different techniques for LPE growthdescribed as,

(1) Nelson method

The substrate is kept on one side of boat and solution on other side in tilted position. Whole boat is inside the quartz tube which in continuously flown by H_2/N_2 gas. Boat has slots for thermocouple and heater. When stable temperature above the saturation level is attained, boat is tilted so that solution covers the substrate and then temperature is reduced. Reducing temperature below solubility limit solution is now supersaturated at that temperature and gets deposited on substrate. The rate of deposition depends on temperature difference from saturation temperature.
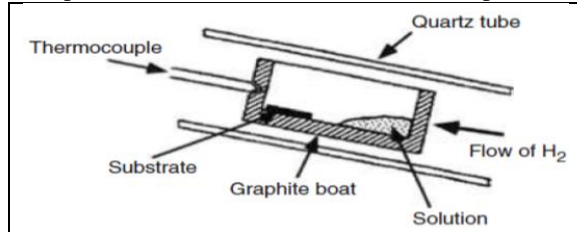
Fig.6 Nelson LPE growth method (peter & Michael, 2007)

(2) Dipping method

This method is similar to Nelson method except for solution is kept in boat and substrate dipped in solution vertically and temperature is reduced under saturation temperature.
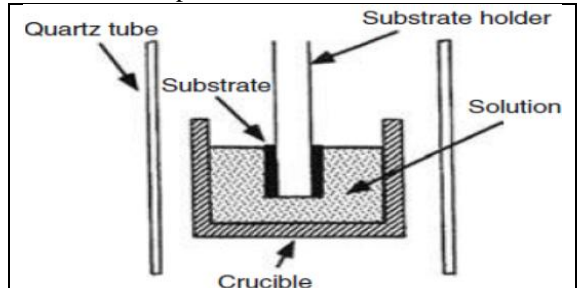
Fig.7 Dipping growth method (peter & Michael, 2007)

(3) Sliding-boat method

This method consists of graphite boat with several slot in which solution is kept. This is most useful method because in this case we can exactly control the thickness of deposited film by sliding the boat, which removes the solution from substrate. This method also allows the deposition of different layer with to make complete device such as diode and semiconductor lasers.
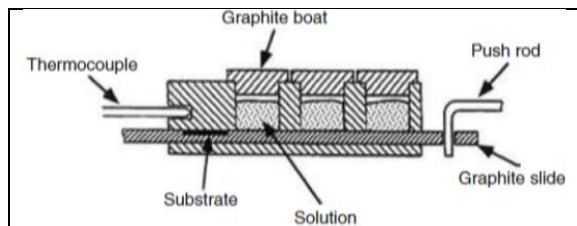
Fig.8 Sliding boat growth method (peter & Michael, 2007)

(4) **Rotating-crucible method**

This method can deposit multi layers of thin film and used to fabricate device. In this method, a shaft rotates centrally with substrate. Substrate is kept in the solution reservoir. Supersaturated solution in solution reservoir gets deposited on substrate.
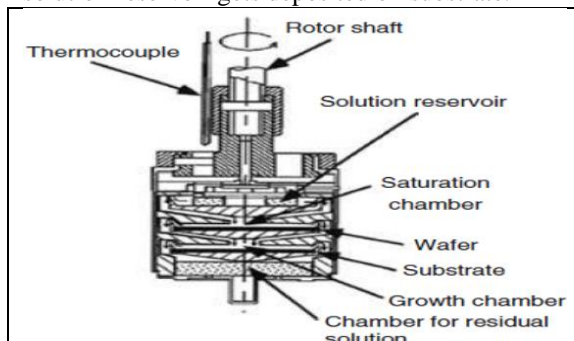
Fig. 9 Rotating crucible growth method (peter & Michael, 2007)

V.   EXPERIMENTAL SECTION

We use Nelson boat technique for PLE deposition (shown in fig 10). In which N_2 gas flows through the quartz tube in which boat is kept. There are three slots for thermocouples in boat, two for substrate and solution thermocouples and third for heater. Boat has also a slot for substrate. Substrate is kept in this slot and solution is dropped on the substrate. Then boat is inserted in glass tube and starts the N_2 gas flow.

(1) **Solution preparation and LPE Heater calibration**

CH_3NH_3I Synthesis: 38mL methylamine (CH_3NH_2) solution (33wt% in absolute ethanol) was reacted dropwise with equimolar (40mL) hydroiodic acid (HI) (57wt % in water) with stirring at 0 °C for about 2 h in ice bath. Crystallization of CH_3NH_3I was achieved using a rotary evaporator. Precipitate was washed three times with diethyl ether at interval of 30 min. finally the precipitate was dried at 60^0C using rotary evaporator.

Prepared methyl ammonium iodide and lead iodide were mixed in **3:1 molar ratio** in organic solvent DMF. The saturation at **75 ^{0}C** was obtained by adding **71.3 wt. %** of solutes in DMF. Also, solution with different wt. % (see supplementary information for saturation point at different wt. % concentration) was prepared to optimize the thickness of deposited film. As lower the concentration of solution, the lower will be the film thickness and higher the saturation temperature. So, we also used high temperature and low concentration to decrease the film thickness.

We also calibrated the heater (see heater calibration part in supplementary information) used for heating the substrate. At each voltage applied from variac to theheater, we measured the voltage generated at thermocouple. The temperature corresponding to

generated voltage at thermocouple is found from standard temperature Vs millivolt chart for specific thermocouple.
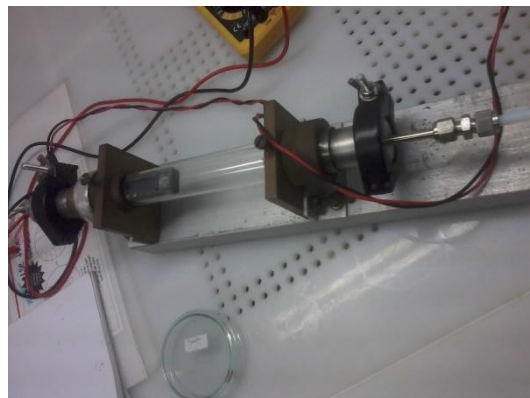
Fig. 10 Experimental Nelson set-up for LPE deposition.

(2) **LPE deposition**

Glass substrates were cut and sonicated with soap water, deionised ion, acetone and isopropyl alcohol for 10 min each. This procedure remove the organic and inorganic impurity from substrate surface. Then heated at 100^0C for 15 min.then cleaned the substrate in plasma cleaner for 10 min at 250 mbarr pressure.This process remove any dust particle left on substrate. Commercial available PDOT:PSS solution in water was ultrasonicated and filtered, then solutionwas spin coated on substrate at 4000 rpm for 60 sec.Then substrate was annealed at 150 ^{0}C for 15 min.Substrate was loaded in boat and solution was dropped on substrate. After passing N_2 gas for 10 minutes so that air is blown out by N_2 gas, to avoid any reaction of hot boat with air. The heater power supply is turned on and voltage correspond to 100 ^{0}C is applied. When solvent was evaporated out sample was taken outside. We also used different type of substrate, silicon, Al deposited glass, gold deposited glass and Ag deposited glass to check the adhesion property of perovskite on different substrates. We also used different concentration of solution to tune the film thickness. As lowering the solution concentration increases the saturation temperature, so we used different deposition temperature as well.

VI.   RESULTS AND DISCUSSION:

(1) **Morphology and coverage of deposited film**

The films are deposited at substrate by LPE at different temperature and annealed at 100 ^{0}C to evaporate the solvent completely. The fig11 describes the deposition parameters. Imaging is done by 100x magnification of Zeta 3D microscope, NCPRE characterization lab at CEN, IITB.As

---

expected, reducing the wt. % from 71.3 to 1 film thickness decreases. The detail of substrate, solution concentration, amount of solution used for deposition, substrate temperature, deposition time and annealing time is given in each subfigure of fig11. Specially in fig 11(c) large crystalline domains of $CH_3NH_3PbI_3$ are seen on the film. Which is due to not allowing the solution to pour below the substrate, in other words solution get enough time to crystallize on substrate surface.
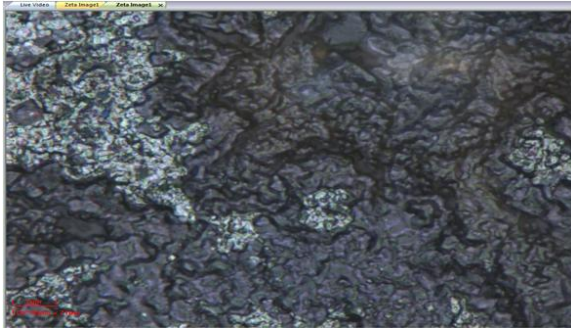
Fig.11(a) Substrate= glass/ PEDOT:PSS, Solute concentration= 71.3 wt% ABI_3 in DMF, Amount of solution = 100 μl, Substrate temp. = 100 ^{0}C, Deposition time = 30 min, Annealed for 15 min.

Fig.11(b) Glass plate was covered on boat to prevent evaporation, Substrate= glass/ 5 nm Al by evaporation, Solute concentration= 55.4 wt% ABI_3 in DMF, Amount of solution = 50 μl, Substrate temp. = 100 ^{0}C, Deposition time = 45 min, annealing time =15 min.
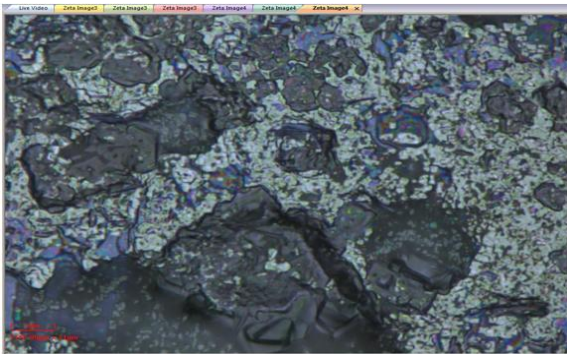
Fig.11(c) Substrate= glass/ PEDOT:PSS, Solute concentration= 40 wt% ABI_3 in DMF, Amount of solution = 40 μl, Deposition time = 1 hour 45 min, Solution was kept on substrate only and didn't allowed to pour below substrate.
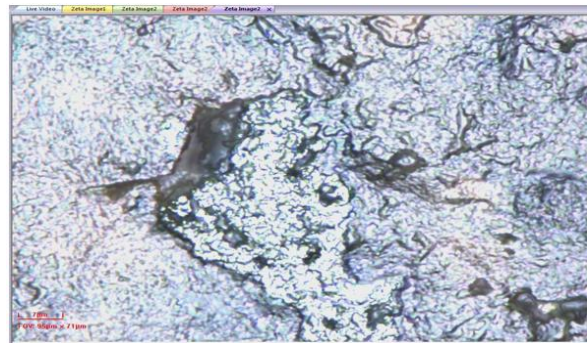
Fig.11(d) Substrate= glass/ PEDOT:PSS, Solute concentration= 19.77 wt% ABI_3 in DMF, Amount of solution = 30 μl, Deposition time = 45 min, Solution was kept on substrate only and didn't allowed to pour below substrate.
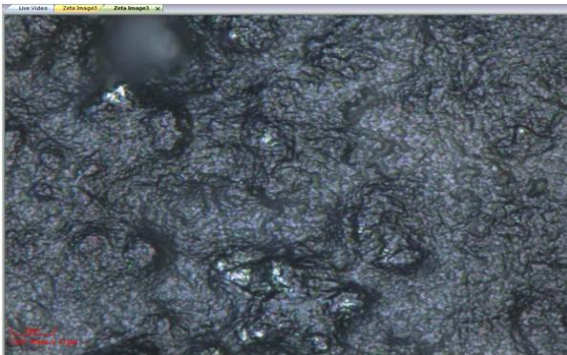
Fig.11(e) Substrate= glass/ PEDOT:PSS, Solute concentration= 11 wt% ABI_3 in DMF, Amount of solution = 20 μl, Deposition time = 30 min, Solution was kept on substrate only and didn't allowed to pour below substrate.
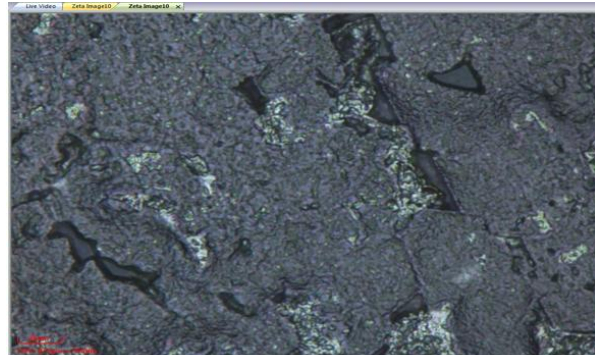
Fig.11(f) Substrate= glass/ PEDOT:PSS, Solute concentration= 4.73 wt% ABI_3 in DMF, Amount of solution = 20 μl, Deposition time = 25 min, Solution was kept on substrate only and didn't allowed to pour below substrate.
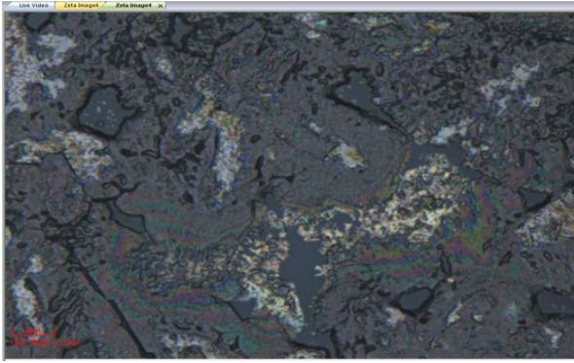
Fig.11(g) Substrate= glass/ PEDOT:PSS, Solute concentration= 1 wt% ABI_3 in DMF, Amount of solution = 30 µl, Deposition time = 35 min, Solution was kept on substrate only and didn't allowed to pour below substrate.
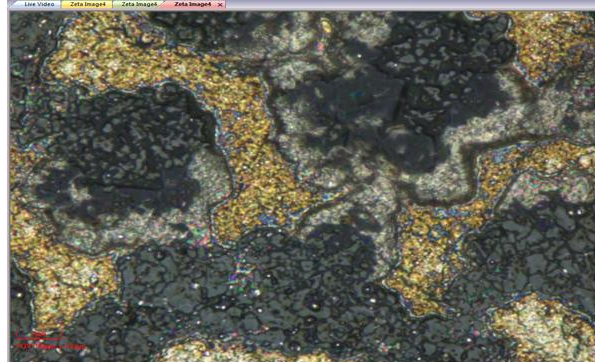
Fig.11(h) Substrate= glass/ 100 nm Ag, Solute concentration= 1 wt% ABI_3 in DMF, Amount of solution = 30 µl, Deposition time = 35 min, Solution was kept on substrate only and didn't allowed to pour below substrate.
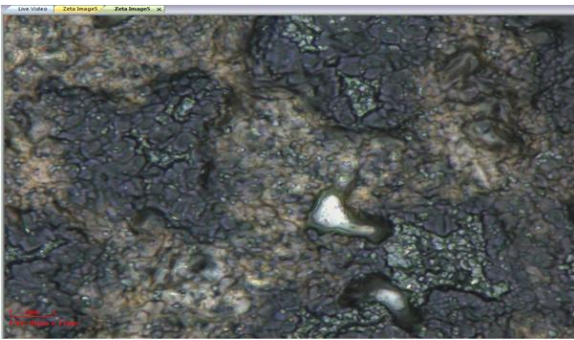
Fig.11(i) Substrate= glass/ 100 nm Ag, Solute concentration= 4.77 wt% ABI_3 in DMF, Amount of solution = 30 µl, Deposition time = 35 min, Solution was kept on substrate only and didn't allowed to pour below substrate.

Fig.11(j) Substrate= glass/ 70 nm Al, Solute concentration= 4.77 wt% ABI_3 in DMF, Amount of solution = 30 µl, Deposition time = 35 min, Solution was kept on substrate only and didn't allowed to pour below substrate.
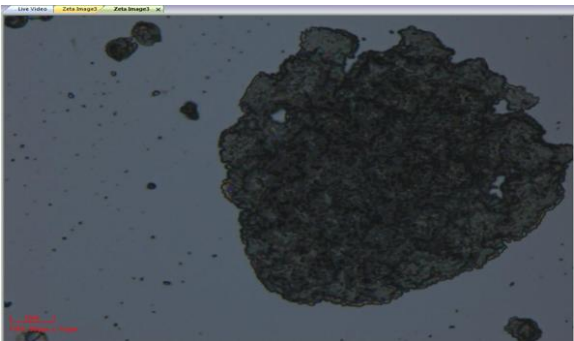
Fig.11(k) Substrate= silicon(100), P type, Solute concentration= 40 wt% ABI_3 in DMF, Amount of solution = 30 µl, Deposition time = 55 min, Solution was kept on substrate only and slid down after 10 min.

From fig 11 (a) and fig11 (b), it seen that covering the covering the boat with glass slow down the evaporation and enhance the crystal quality. From fig 11 (c) and fig 11 (d), it is seen that decreasing the concentration smoothens the film with cost of decrease in crystallinity. Comparing fig 11(e) and fig 11(f), we see that reducing the concentration further, smoothen the film. We also see the pin holes in the fig 11(f) film which indicate the poor coverage due to very low concentration.Pin hole are even more in fig 11(g), which is not good for optoelectronic device application.100 nm thermally evaporated, Ag coated glass substrate was used in fig 11(h), but we see that some parts are shiny and having totally different color than perovskite. This indicates that perovskite may reacted with Ag, which is not good

for perovskite layer deposition. While in fig 11(i), we see tha same Ag film with higher concentration of perovskite, 4.77 gives less defective film, which concludes that Ag react with perovskite, but with 1 wt% solution 100 nm Ag is enough to disrupt the film but as concentration was increased to 4.77, for this thicker film, 100 nm Ag is not stuffiest to react much. In fig 11(j), 70nm Al thermally evaporate glass substrate was used and solution concentration was 4.77 wt%. We see that even 70 nm Al is sufficient to react with 4.77 wt % film, which indicate that Al react more with perovskite than with Ag. In fig 11(k) we used cleaned silicon (100), P-type as substrate. We found that the adhesion of perovskite with silicon is very poor and it forms patches of perovskites.

(2) X-ray diffraction

X-ray diffraction were done by HRXRD (by RigakuSmartlab 3KW diffractometer) using Cu K_α (λ =1.54 Å). all peaks position are matching with literature(Tian & Scheblykin 2015). Intensity of second peak found higher than first one, which is due to excess amount of CH_3NH_3I. Also, there is no sign for PbI_2 peak at 14^0. In sample 1 100 microliter solution was used while in sample2 200 microliters.
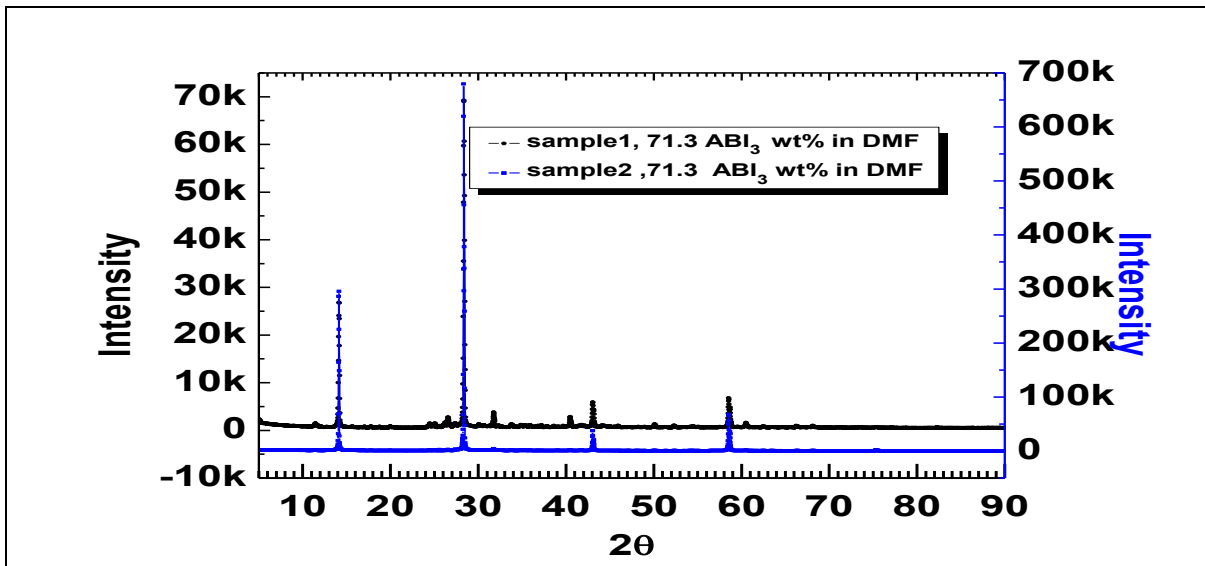
Fig 12: X-ray Diffraction of two LPE deposited film with 71.3 wt % $CH_3NH_3PbI_3$ in MDF.

Comparing with literature(Jeon et al. 2014), peaks are matching and small value of FWHM indicating highly crystalline nature of thin film.

Plane	Sample (1) [2θ]	Sample (2) [2θ]	FWHM (1) [2θ]	FWHM (2) [2θ]
(110)	14.15	14.11	0.11	0.11
(220)	28.38	28.35	0.15	0.12
(312)	31.78	31.74	0.12	0.12
(224)	40.48	40.49	0.13	0.10
(314)	43.06	43.05	0.10	0.10
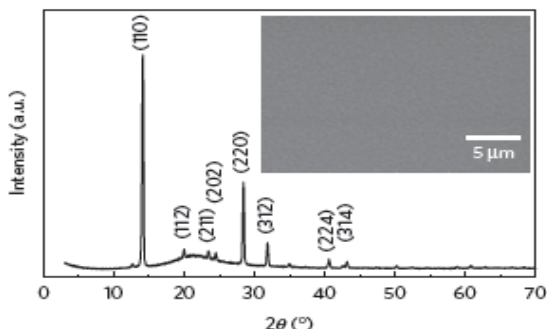
Fig.13 XRD plot of ABI_3 from literature(Jeon et al. 2014)

(3) UV-Vis-NIR Spectroscopy

Absorption spectroscopy was taken by PerkinElmer LAMBDA 950. Film is absorbing whole range of visible spectra right from 800 nm. Absorption spectra have lot of artefact and resemble with indivisible crystal spectra(Tian & Scheblykin 2015). Spectra are matching with reported spectra(Malinkiewicz et al. 2014).
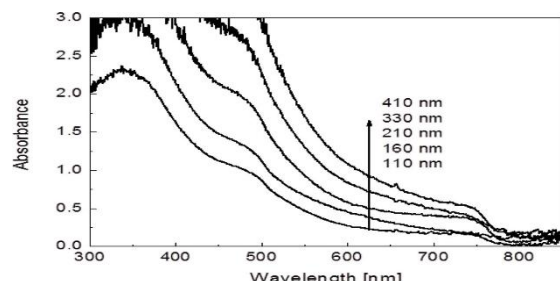
Fig.15 UV-Vis spectra of $CH_3NH_3PbI_3$ taken from literature (Tian & Scheblykin 2015).

There is gradual increase in absorbance in wavelength lower than 780 nm. Excitonic peak near band edge is not visible in the graph. The O.D. saturates at wavelengthlower than 400 as thickness is toohigh hence data lower than 400 nm is not relevant.

VII. SUMMARY

We have seen that liquid phase epitaxy method gives large grain size, crystalline perovskite thin film. Hybrid halide perovskite materials have high tendency for crystallisation.As optoelectronic properties of material highly depend on crystalline nature and for solar cell application, we need the bigger grain for better charge mobility, LPE is the promising technique for bigger grain or single crystalline. The grain size of as long as 7 μm was achieved with this technique and can be improved a lot. As the perovskite react with Ag and Al, so it is not good to deposit the film on these substrates. It also implies that if Ag/Al will be used as electrode in solar cells then it might degrade the performance. We are getting better coverage and lower thickness with at lower concentration of solute which is required for solar cell application. It is seen that PEDOT: PSS coated substrate give better coverage than other metal deposited substrates. We also see that perovskite grains are big enough on silicon substrate as well, which can be further enhanced. For the perovskite on silicon tandem solar cells, LPE can be better technique to deposit crystalline film with larger grain size.

ACKNOWLEDGMENT

REFERENCES

1. Akihiro Kojima, K. T. Y. S. a. T. M., 2009. Organometal Halide Perovskites as Visible-Light Sensitizers for Photovoltaic Cells. *J. AM. CHEM. SOC. 2009, 131, 6050–6051.*

2. Chonghea Li, X. L. W. D. L. F. Y. G. a. Z. G., 2008. Formability of ABX3 (X = F, Cl, Br, I) halide perovskites. *Acta Cryst. (2008). B64, 702–707.*

3. E. Mosconi, A. A. M. K. N. M. G. a. F. D. A., 2013. *J Phys Chem C, 2013, 117,13902-13913.*

4. Edoardo Mosconi, A. A. M. K. N. M. G. a. F. D. A., 2013. First-Principles Modeling of Mixed Halide Organometal Perovskites for Photovoltaic Applications. *dx.doi.org/10.1021/jp4048659 | J. Phys. Chem. C 2013, 117, 13902−13913.*

5. Guichuan Xing, e., 2013. Long-Range Balanced Electron and Hole-Transport Lengths in Organic-Inorganic CH3NH3PbI3. *Science, 2013, 342, 344-347..*

6. Mathews, T. C. S. a. N., 2014. Advancements in Perovskite Solar Cells: Photophysics behind the Photovoltaics. *DOI: 10.1039/C4EE00673A,* p. 1.

7. Peter, c. & Michael, m., 2007. *Liquid Phase Epitax of electronic, optical and optoelectronic material.* s.l.:John Wiley & Sons Ltd.

8. Samuel D. Stranks, G. E. E. G. G. C. M. J. P. A. T. L. L. M. H. A. P. H. J. S., 2013. Electron-Hole Diffusion Lengths Exceeding 1 Micrometer in an Organometal Trihalide Perovskite Absorber. *SCIENCE VOL 342 18 OCTOBER 2013.*

9. Valerio D'Innocenzo, G. G. M. J. A. A. R. S. K., 2014. Excitons versus free charges in organo-lead tri-halide perovskites. *DOI: 10.1038/ncomms4586.*